Article

Trajectory of Spike-Specific B Cells Elicited by Two Doses of BNT162b2 mRNA Vaccine

Annalisa Ciabattini[1*], Gabiria Pastore[1], Simone Lucchesi[1], Giorgio Montesi[1], Simone Costagli[1], Jacopo Polvere[1], Fabio Fiorino[1,2], Elena Pettini[1], Arianna Lippi[3,4], Leonardo Ancillotti[3,4], Mario Tumbarello[3,4], Massimiliano Fabbiani[3], Francesca Montagnani[3,4] and Donata Medaglini[1]

[1] Laboratory of Molecular Microbiology and Biotechnology, Department of Medical Biotechnologies, University of Siena; Siena, Italy
[2] Department of medicine and Surgery, LUM University, Casamassima (Bari), Italy
[3] Department of Medical Sciences, Infectious and Tropical Diseases Unit, University Hospital of Siena; Siena, Italy
[4] Department of Medical Biotechnologies, University of Siena; Siena, Italy
* Correspondence: annalisa.ciabattini@unisi.it

Abstract: The mRNA vaccines for SARS-CoV-2 have demonstrated efficacy and immunogenicity in the real-world setting. However, most of the research on vaccine immunogenicity has been centered on characterizing the antibody response, with limited exploration into the persistence of spike-specific memory B cell response. Here we monitored the durability of the memory B cell response and characterize the trajectory of spike-specific B cell phenotypes in healthy individuals who have received two doses of the BNT162b2 vaccine up to 9 months post-vaccination. To profile the spike-specific B cell response we applied the tSNE and Cytotree automated approaches. Our data showed the induction of spike-specific IgA^+ and IgG^+ plasmablasts and IgA^+ activated cells 7 days after the second dose which disappeared 3 months later, while subsets of spike-specific IgG^+ resting memory B cells became predominant 9 months after vaccination, and they were capable to differentiate into spike-specific IgG secreting cells when in vitro restimulated. Other subsets of spike-specific B cells, such as IgM^+ or unswitched IgM^+IgD^+ or IgG^+ double negative/atypical cells, were also elicited by the BNT162b2 vaccine and persisted up to month 9. The analysis of circulating spike-specific IgG, IgA and IgM was in line with the plasmablasts observed.
The longitudinal analysis of the antigen-specific B cell response elicited by mRNA-based vaccines provides valuable insights into our understanding of the immunogenicity of this novel vaccine platform destined to a future widespread use, and it is crucial in guiding future decisions and vaccination schedules.

Keywords: B cell response; mRNA vaccination; computational analysis; SARS-CoV-2; COVID-19

1. Introduction

The COVID-19 pandemic has affected millions of people worldwide, causing significant morbidity and mortality (https://covid19.who.int/). Vaccination has emerged as a crucial strategy in restraining the severity of the disease, and several vaccines have been developed to combat the COVID-19 virus. These vaccines, employing different mechanisms of action, have shown varying levels of efficacy and safety [1]. Among these, RNA technology represents a revolution in vaccine production as it enables faster and less expensive production compared to traditional methods, and can be easily adapted to address virus mutations. RNA vaccines are expected to remain a critical approach in the fight against infectious diseases, not only for COVID-19, but also for other pathogens such as influenza, HIV, as well as for non-infectious diseases such as cancer and autoimmune disorders [2–5]. However, further research is still needed to fully evaluate the immunogenicity, safety, and efficacy of this technology. A critical question surrounding COVID-

 doi:10.20944/preprints202305.1190.v1

19 vaccination with mRNA-based vaccines is the duration of the immune response elicited. Current evidence suggests that vaccinated individuals maintain robust protection against severe illness and mortality for a minimum of 6 months [6]. However, the effectiveness of the vaccines in preventing infection and mild symptoms may diminish over time [7]. Consequently, public health agencies have recommended the administration of booster doses, starting 4-6 months after completing the primary vaccination series, to enhance protection against severe illness and death caused by COVID-19. Older and vulnerable populations have been prioritized for booster immunization due to their pathologies or immunosuppressive treatments that compromised immune responsiveness [8–13]. Numerous studies have demonstrated the critical role of the third vaccine dose for vulnerable individuals, such as those with myelofibrosis, undergoing haemodialysis, or recipients of hematopoietic cell transplants, who exhibited a weaker or slower immune response to the initial vaccination cycle [11,14–17]. Despite strong recommendations for the third dose, as of May 2023, only 30% of the global population has received the booster dose, while 65.5% of people have completed the primary vaccination cycle with two doses [https://covid19.who.int/table]. Therefore, it is crucial to investigate the persistence of immune memory following the initial vaccination schedule. Additionally, as mRNA-based platforms are being used for the first time, various aspects regarding the safety, mechanisms of action of the nanoparticles [18] and the antibody response have been extensively examined from the outset in both healthy and fragile subjects [13,19,20]. However, other aspects, such as the long-term persistence of immune memory [21–24] and the hybrid immunity induced by concurrent viral infection [25,26], remain under investigation and necessitate continuous updates.

Immune memory is the immunological mechanism that protects individuals against reinfection. It is the primary target of vaccination, as memory B cells (MBCs) can rapidly reengage upon re-encountering the antigen, differentiating into antibody-secreting cells capable of combating microbial infections [27]. Long-lived plasma cells, originating from the germinal center and residing in the bone marrow, are also integral components of the memory cell pool [28]. These cells exhibit higher antibody avidity and secretion rates compared to their short-lived counterparts generated primarily through extrafollicular reactions. Vaccination also induces memory T cells, as observed with numerous COVID-19 vaccines [29–31], and reactivated memory T cells are able to kill infected cells, thus preventing viral multiplication and spread. SARS-CoV-2 infection and/or vaccination studies have revealed the persistence of memory cells in unvaccinated infected patients [32–34] and vaccinated subjects [21,23,24,31,35] when antibody levels naturally decline over time. In a previous work, we demonstrated the generation and persistence of peripheral spike-specific MBC and circulating antibodies up to 6 months after the first cycle of vaccination with the BNT162b2 vaccine in a cohort of SARS-CoV-2-naïve healthy subjects [35]. Furthermore, the long-term persistence of germinal center reaction into axillary draining lymph nodes, together with the generation of high affinity-MBCs and long-lived plasma cells, has been demonstrated in humans who received the two-dose series of BNT162b2 vaccination [36].

Here, we characterized the temporal dynamics and magnitude of the spike-specific B cell response in a cohort of healthy subjects following the administration of the second dose of the BNT162b2 mRNA vaccine over a 9-month period post-vaccination. Notably, this cohort was selected based on the absence of nucleocapsid-specific antibodies at all analyzed time points, making it an ideal population for profiling the antigen-specific B cell response specifically induced by the novel mRNA-based vaccination platform, independent of any confounding effects of hybrid immunity resulting from natural infection.

2. Materials and Methods

2.1. Study design

 doi:10.20944/preprints202305.1190.v1

Plasma and peripheral blood mononuclear cells (PBMCs) samples were obtained from a total of 30 healthcare workers (HCWs) aged 26-63 years who received two doses of the BNT162b2 (Pfizer-BioNTech; Comirnaty) vaccine, 3 weeks apart. Exclusion criteria included pregnancy, previous documented SARS-CoV-2 infection and immunocompromising comorbidities (congenital, acquired or drug-related). All participants provided written informed consent before participation to the study. Study participants were recruited at the Infectious and Tropical Diseases Unit, Azienda Ospedaliera Universitaria Senese (Siena, Italy). The study was performed in compliance with all relevant ethical regulations and the protocol was approved by local Ethical Committee for Clinical experimentation of Regione Toscana Area Vasta Sud Est (CEAVSE), protocol code 18869 IMMUNO_COV v1.0 of 18 November 2020, approved on the 21 December 2020. Clinical data collection and management were carried out using the software REDCap (Research Electronic Data Capture, Vanderbilt University).

2.2. PBMCs isolation

Venous blood samples were collected in heparin-coated blood tubes (BD Vacutainer). PBMCs were isolated by density-gradient sedimentation, using Ficoll-Paque (Lymphoprep, Meda, Italy). Cells were gently resuspended with warm cell recovery medium [10% DMSO (Thermo Fisher Scientific) and 90% heat inactivated fetal bovine serum (Sigma Aldrich)] and then rapidly transferred to cryovials that were incubated o.n. at -80°C using an isopropanol freezing container. Vials were cryopreserved in liquid nitrogen. Plasma samples were stored at −80°C. Serological and flow cytometry analysis were performed in frozen/thawed samples.

2.3. Multiparametric flow cytometry

SARS-CoV-2-specific B cells were identified and characterized among thawed PBMC by flow cytometry. Biotinylated Spike S1+S2 ECD-His protein (Sino Biological) and RBD domain (BioLegend) were tetramerized with streptavidin (SA) fluorescently labeled with R-Phycoerythrin (PE; Thermofisher) or Allophycocyanin (APC; Thermofisher), as previously described [37]. Briefly, 2 millions of PBMCs were blocked with BD human FC block (BD Biosciences), and stained for 30 min at 4°C with the following antibody-fluorochrome panel: CD3-BV650 (clone SK7); CD19-BUV395 (clone SJ25C1), IgM-BV605 (clone G20-127), IgD-BV711 (clone IA6-2), CD20-APC-H7 (clone 2H7), CD27-BV786 (clone M-T271), CD21-FITC (clone B-ly4), CD38-BUV737 (clone HB7), IgG-PE-Cy7 (clone G18-145, all from Becton Dickinson), IgA-VioBlue (clone IS11-8E10, Miltenyi Biotec). After staining cells were labeled with Zombie Aqua™ Fixable Viability Kit (Thermofisher) according to the manufacturer instruction, and fixed with BD fixation solution (BD Biosciences). All antibodies were titrated for optimal dilution. About 1×10^6 cells were acquired for each sample with SO LSRFortessa X20 flow cytometer (BD Biosciences). Manual data analysis was performed using FlowJo v10.8.1 (TreeStar, USA).

2.4. t-SNE analysis

The B cell population analyzed was gated as live, singlet, $CD3^-/CD19^{+/low}$ cells using FlowJo v10 (TreeStar, USA) For each sample was randomly sampled an equal amount of cells (n=5000) and for each time point was selected an equal number of samples (n=12), then B cell files were exported from FlowJo as uncompensated flow cytometry standard (FCS) file. FCS files were imported in R environment (v4.1.3) as flowSet object, that was then compensated with FlowCore package 2.6.0 [38] and logicle transformed [39]. t-Distributed Stochastic Neighbor Embedding (t-SNE) [40] dimensionality reduction was performed with Rtsne package v0.15. Expression values of each marker were normalized as z-scores (mean=0 and standard deviation=1), then t-SNE algorithm was run setting perplexity = 100, selected as optimal parameter value in a range between 5 and 200. B cells were also manually analyzed with FlowJo, and labels of different B cell populations were

 doi:10.20944/preprints202305.1190.v1

imported in R environment using GetFlowJoLabels function from FlowSOM package (v2.2.0) [41]. Contour plot of individual B cell populations were displayed with the function Contour from FlowViz package (v1.58.0).

2.5. Trajectory analysis

Spike$^+$ RBD$^+$ cells were imported in R environment as compensated FCS files. Quality control, normalization and sample merging were all performed using CytoTree package (v1.0.3) [42]. After correcting for batch effect using the sva package (v3.46.0) [43], unsupervised clustering was performed using FlowSom package (v2.2.0) and 36 clusters and 9 meta clusters were set up. The t-SNE dimensionality reduction was applied to both cells and clusters to construct trajectories for all clusters using a Minimum Spanning Tree approach implemented in CytoTree. The analysis of differentially expressed markers, including CD27, CD21, CD20, CD19, CD38, IgA, IgD, IgM and IgG performed using both CytoTree and flowDensity (v1.32.0) [44], allowed the identification of the different cellular phenotypes present within the Spike$^+$ RBD$^+$ population.

2.6. B-cell ELISpot

PBMCs, collected from subjects 9 months following vaccination, were evaluated for IgG production using Human IgG Single-Color Enzymatic ELISpot assay (CTL Europe GmbH, Bonn, Germany). The protocol was performed according to the manufacturer instruction. Briefly, 2×10^6 PBMCs/ml were stimulated with polyclonal B cell Stimulator for 4 days, and then cells were transferred on multiscreen filter 96 well plates, coated with recombinant wild type SARS-CoV-2 Spike S1+S2 (Sino Biological, 10 µg/ml) or anti-Ig capture antibody or un unrelated antigen, and incubated o.n. Plates were then incubated with anti-human IgG detection solution, and with Tertiary Solution and developed by adding Blue Developer Solutions. The number of spots was determined by plate scanning and analysed with an Immunospot S6 Ultimate Analyzer (CTL Europe GmbH).

2.7. ELISA and ACE2/RBD inhibition assay

Maxisorp microtiter plates (Nunc, Denmark) were coated with recombinant wild type SARS-CoV-2 Spike S1+S2 ECD (Sino Biological), as previously described [14], or with the SARS-CoV-2 nucleoprotein (1 µg/ml, Sino Biological). Briefly, after blocking plates were added with plasma samples for 1 h at RT. Anti-human horseradish peroxidase (HRP)-conjugated IgG (diluted 1:6000), IgM (diluted 1:2000) or IgA (diluted 1:4000; all from Southern Biotech) were added for 1 h and plates were developed with 3,3',5,5'-Tetramethylbenzidine (TMB; Thermo Fisher Scientific) substrate. Absorbance at 450 nm was measured on Multiskan FC Microplate Photometer (Thermo Fisher Scientific). WHO international positive (NIBSC 20/150 and 20/144 for S and N, respectively) and negative (NIBSC 20/142) controls were added in duplicate to each plate as internal controls for assay reproducibility and to set the positive threshold.

ACE2/RBD inhibition was tested with a SARS-CoV-2 surrogate virus neutralization test (sVNT) kit (cPass™, Genscript), according to the manufacturer protocol, as already described [35]. Briefly, diluted plasma samples, positive and negative controls were mixed 1:1 with diluted HRP-RBD (either Wuhan, Delta or Omicron BA.1 variants, Sino Biologicals) for 30 min at 37°C, and then each mixture was added to ACE2-coated flat-bottom 96 well plates. TMB solution were added to each well and plates were developed for 15 min at RT. The adsorbance was measured at 450 nm on Multiskan FC Microplate Photometer (Thermo Fisher Scientific). Results of the ACE2/RBD inhibition assay are expressed as percentage inhibition = (1 - sample OD value/negative control OD value) * 100. Inhibition values ≥30% are regarded as positive results, as indicated by the manufacturer.

2.8. Statistics

Preprints (www.preprints.org) | NOT PEER-REVIEWED | Posted: 17 May 2023 doi:10.20944/preprints202305.1190.v1

Kruskall-Wallis test, followed by Dunn's post test for multiple comparative tests was used for assessing statistical between frequencies of S^+RBD^+ B cells and subsets at different time points. Mann–Whitney test was used for assessing statistical difference between Spike-specific and unrelated antigen-specific B cells in ELISPOT data. A P-value ≤ 0.05 was considered significant. Analyses were performed using GraphPad Prism v9 (GraphPad Software, USA).

3. Results

3.1. Durability of Spike-specific memory B cells overtime

The spike-specific B cell response in healthy subjects vaccinated with two doses of the BNT162b2 mRNA vaccine, was analysed starting from 7 days up to 9 months after second dose administration. To exclude a booster effect elicited by a possible SARS-CoV-2 infection, all participants were assessed for anti-nucleoprotein antibodies at all time points, and only subjects with negative results were included in the present study (Supplementary figure 1).

SARS-CoV-2 specific B cells were identified among $CD19^{+/low}$ cells by the simultaneous labeling with the spike and RBD probes coupled to different fluorescent dyes (hereafter named S^+RBD^+ B cells; Figure 1 a). S^+ RBD^+ B cells cells were significantly elicited by vaccination, increasing from 0% at day 0 to 0.15% ± 0.1 of total $CD19^{+/low}$ B cells at day 7 after the second vaccine dose (P<0.001). The frequency of S^+ RBD^+ B cells increased overtime, reaching values of 0.31% 9 months after vaccination (P<0.001 versus day 0, Fig. 1 b). Circulating B cells at month 9 were able to reactivate upon in vitro restimulation and secrete spike-specific IgG, as assessed by memory B-cell ELISpot assay. Reactivated memory B cells secreting spike-specific IgG were detected in 82% of the tested subjects, with a mean value of 0.6% of spike-specific secreting IgG respect to total IgG (Figure 1 c).

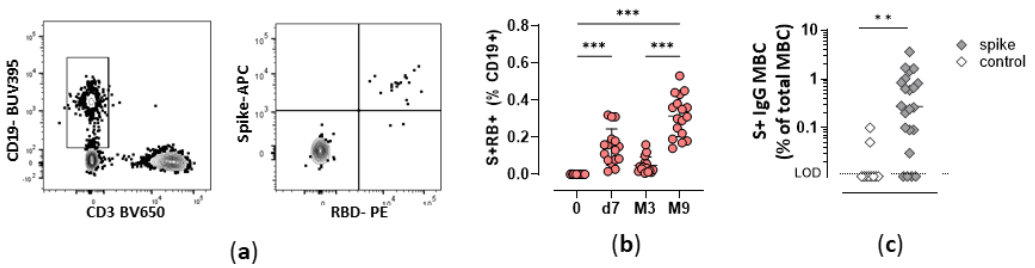

Figure 1. Spike-specific B cells in vaccinated subjects (**a**) Flow cytometry analysis of S^+RBD^+ cells gated on live $CD19^{+/low}$ cells, and (**b**) their frequency at baseline (0), 7 days (d7), 3 (M3) and 9 (M9) months after the second vaccine dose; Kruskall-Wallis test, followed by Dunn's post test for multiple comparative tests was used for assessing statistical differences between cell frequency at different time points. ***P≤ 0.001. (**c**) spike-pecific IgG producing cells, assessed by B-cell ELISPOT upon in vitro restimulation of PBMC collected at month 9 ; production of IgG against un unrelated antigen (control) is also shown. The dotted line indicates the limit of detection (LOD). Mann–Whitney test, was used for assessing statistical differences between groups. **P≤ 0.01.

3.2. Trajectory analysis of Spike-specific B cells at different time points

A deep phenotypic longitudinal analysis of total and S^+ RBD^+ B cells was performed to define the trajectory of spike-specific B cell response up to 9 months after vaccination. Our flow cytometric analysis was based on a panel that included markers for identifying plasmablasts and different MBCs subsets (CD19, CD20, CD21, CD38 and CD27), as well as the major Ig isotypes (IgD, IgM, IgG, and IgA). A manual gating analysis was firstly performed using CD27, CD21, IgG, IgA, IgM and IgD markers of all individuals at all time points for defining B cell subsets that were then combined with t-Distributed Stochastic Neighbour Embedding (t-SNE) dimensionality reduction algorithm, a tool which groups

Preprints (www.preprints.org) | NOT PEER-REVIEWED | Posted: 17 May 2023 doi:10.20944/preprints202305.1190.v1

cells in a bi-dimensional map based on phenotype similarity thus providing an intuitive and easy approach to view organization of cell subsets **[45,46].**

The manual analysis of IgD vs CD27 expression allows to identify naïve (IgD^+CD27^-) from antigen-experienced B cells which persist as unswitched (IgD^+CD27^+) or Ig-switched (IgD^-CD27^+), and a double negative subset (IgD^-CD27^-). Similar subsets can be identified by analysing the expression of CD27 vs CD21. Activated ($CD27^+CD21^-$) and resting ($CD27^+CD21^+$) B cells can be distinguished by naïve ($CD27^-CD21^+$) and atypical ($CD27^-CD21^-$) cells. The surface BCR varied from IgD and IgM double positive cells, to Ig-switched subsets that included IgM (only), IgA or IgG positive cells (Supplementary Figure 2).

To gain a global picture of the different B cells subsets and compare S^+RBD^+ B cells at different time points, we import the manual analysis into the tSNE map (Figure 2 a). Different subsets of total B cells were distributed in different area of the map. IgD^+ $CD27^-$ naïve B cells occupied a predominant area of the tSNE map, and most of them were $CD21^+$ and IgD^+ IgM^+ (figure 2a, panels a, b and c respectively). Switched memory B cells were grouped in the right part of the tSNE map (figure 2a, panel a) and included both IgG^+ and IgA^+, with a small fraction of IgM^+ (figure 2a, panel c). Double negative (DN, IgD^-CD27^-) cells included both $CD21^+$ and $CD21^-$ subsets (Figue2 a, panel b) and were IgG^+ (Figue2 a, panel c). The S^+RBD^+ B cells scattered in different regions of the tSNE map, according to the three time points analysed (Figure 2 b, red dots). The distribution and the amount of S^+ RBD^+ B cells changed overtime, suggesting both a quantitative and qualitative modulation of spike-specific B cells 7 days, 3 and 9 months after vaccine administration.

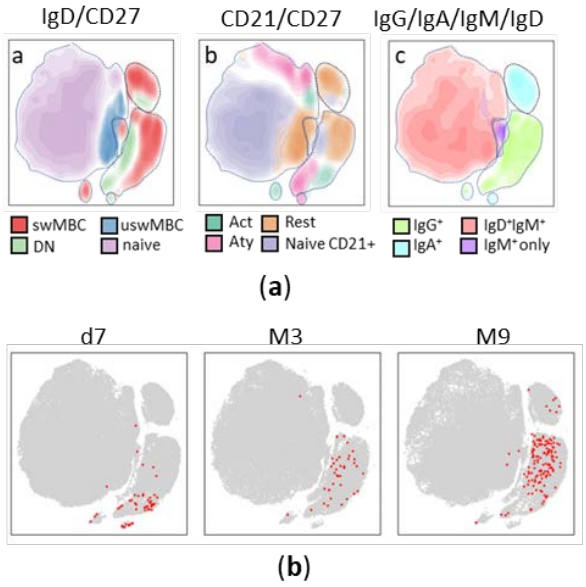

Figure 2. t-SNE analysis of B cell subpopulations and antigen-specific B cells at different time points. a) Different cell subpopulations, according to the expression of different surface molecules, displayed in t-SNE map. The left panel displays major B cell subsets according to CD27 and IgD (switched memory, swM; unswitched memory uswM; double negative, DN; and naïve), middle panel reports B cell subsets according to CD27 and CD21 (activated memory, Act; resting memory, Rest; atypical, Aty; naïve CD21+), right panel reports surface immunoglobulins. b) S^+RBD^+ B cells highlighted as red dots in t-SNE dimensionality reduced map, 7 days (d7), 3 and 9 months after the second vaccine dose (M3 and M9 respectively).

To deeply understand the phenotypes of antigen-specific B cells and their modulation overtime we performed unsupervised consensus hierarchical clustering analysis implemented into the CytoTree package (Fig. 3 a). The computational analysis was performed only on S^+RBD^+ B cells, that were clustered into 36 nodes according to the

Preprints (www.preprints.org) | NOT PEER-REVIEWED | Posted: 17 May 2023 doi:10.20944/preprints202305.1190.v1

expression of CD20, CD38, CD27, CD19, CD21, IgG, IgA, IgM and IgD markers. Phenotypically similar nodes were grouped into 9 metaclusters, colored with the same background, as shown in the tree reported in Figure 3 a. The specific expression of each marker within the metaclusters is shown in the heatmap of Figure 3 b. Metaclusters included IgA$^+$ or IgG $^+$ plasmablasts (PB), activated or resting MBC, IgM$^+$ only resting MBC, IgG$^+$ DN/atypical B cells, and IgD$^+$IgM$^+$ unswitched resting MBC.

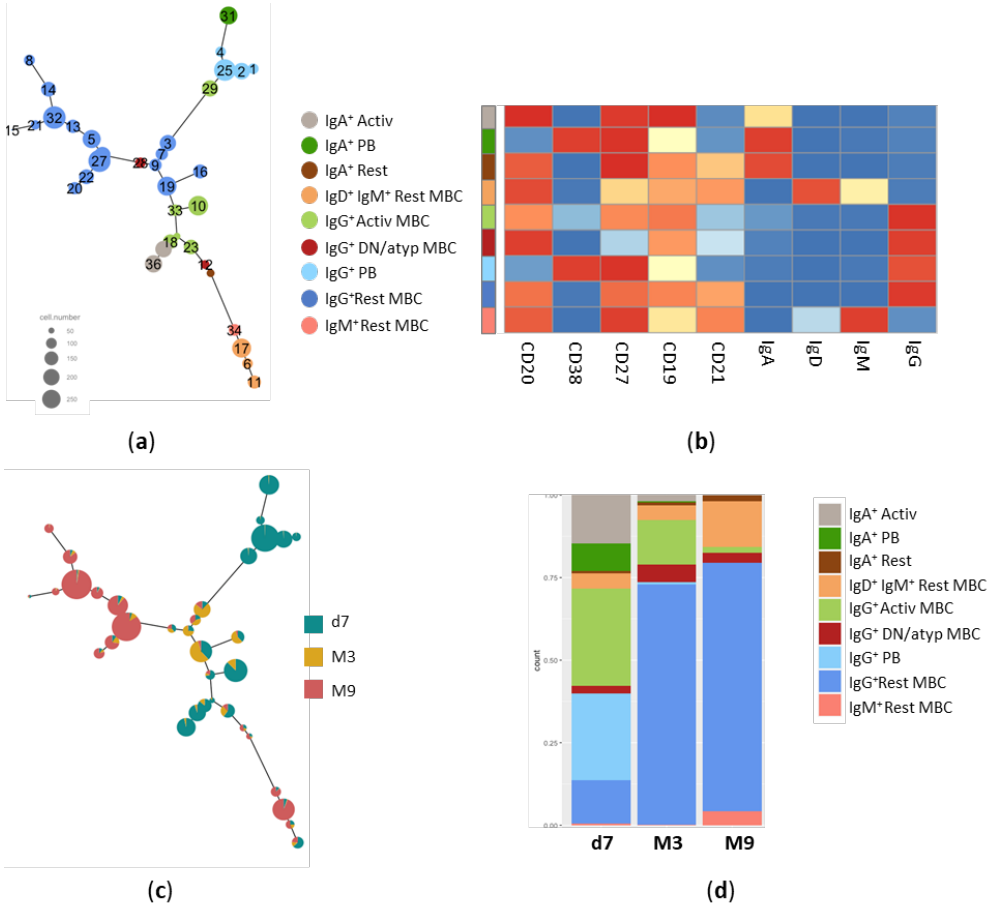

Figure 3. Trajectory analysis of S$^+$RBD$^+$ B cells. (**a**) Minimum Spanning Tree (MST) of FlowSOM clusters obtained from S$^+$RBD$^+$ B cells starting from their t-SNE coordinates using CytoTree. Clusters are colored according to their membershib in the 9 metaclusters. Size of the nodes is relative to the percentage of cells present in each cluster, as reported on the left. (**b**) Heatmap of markers expression within the nine metaclusters. (**c**) Distribution of cells collected at day 7 (d7), 3 (M3) or 9 (M9) months after vaccination within each cluster identified in the MST of panel a. (**d**) Frequency of different phenotypes among S+RBD+ B cells at day 7 (D7), 3 (M3) and 9 (M9) months after vaccination.

Cells of the different time points fell into the different nodes, as shown in figure 3 c. This visualization of the tree clearly highlights the trajectory of the spike-specific B cell phenotypes across the different time points. While IgA$^+$ and IgG$^+$ PB (nodes 1, 2, 4, 31 and 29 of Figure 3 a) and IgA$^+$ activated cells (nodes 36 and 18) were present at day 7 after vaccine administration and then disappeared at 3 and 9 months, subsets of IgG$^+$ activated MBC (nodes 23, 33, and 10) and some clusters of IgG$^+$ resting MBC (nodes 3, 7, 9, 19, 16) were detectable both at day 7 and persist at month 3, while other clusters of IgG$^+$ resting MBC (8, 14, 15, 21, 32, 13, 5, 27, 22,20) were strongly detectable only 9 months after vaccination (Figure 3 b). Some subsets expressing IgM only (node 34), unswitched-Ig (nodes 17, 6 and 11) or DN/atypical B cells (node 28) were detectable from day 7 and persisted up to month 9. The longitudinal analysis clearly showed a trajectory of the different metaclusters over time, with many of them exhibiting alternative expressions between the early

Preprints (www.preprints.org) | NOT PEER-REVIEWED | Posted: 17 May 2023 doi:10.20944/preprints202305.1190.v1

time point (day 7) and the long-term time points (M9; Figure 3 b). The relative frequency of the spike-specific B cell within each metacluster at day 7, month 3 and 9 is shown in Figure 3 d.

In summary, two doses of mRNA vaccine promote a S^+RBD^+-specific B cell response that evolves overtime persisting in blood 9 months after vaccination. Spike-specific PB, both IgA^+ and IgG^+ were detectable only at day 7, while IgA^+ and IgG^+ activated cells were rapidly elicited, downmodulated at month 3 and almost undetectable at month 9. The persistent RBD-specific B cells were dominated by IgG^+ resting MBC phenotype, with a small fraction of IgM^+ IgD^+ unswitched and IgM^+ only cells still circulating.

3.3. Analysis of the Spike-specific IgG response

Concomitant to the development of the S^+RBD^+ B cell response, the induction and persistence of humoral response was assessed. Spike-specific IgM, IgA and IgG were longitudinally analyzed (Figure 4 a). As expected, the spike-specific humoral response peaked at day 7, declined at month 3 and then stably persisted at month 9. Spike-specific IgG were predominant in each subjects, with a peak of 22185 GMT (95% CI 19283 to 31619; range 1280-163840; P≤ 0.001 versus baseline) after vaccine administration and a value of 5120 (95% CI 2951 to 6280; range 1280-20480; P≤ 0.001 versus baseline) at month 9 (Figure 4 a). A very similar trend, but with lower titres was observed for IgM and IgA antibody response, with a peak of 564 and 1177 GMT at day 7 respectively, and a GMT value of 332 at month 9 (Figure 4 a). The induction of IgA and IgG were in line with the detection of IgA^+ and IgG^+ PB observed in Figure 3, while the lack of IgM^+ PB can be due to a very rapid production of IgM^+ short live plasmacells 7-14 days after the first vaccine dose, with a rapid decline. Unfortunately, a cut-off value of circulating antibodies correlating with protection has not been yet identified, also due to the continuous mutation of the virus and the capacity of variants to partially escape the antibody response elicited by vaccination. What we observed in terms of antibody functionality was that in 80% of subjects the antibdies were able to ihibit the binding between wild type RBD and ACE-2 receptor, while 54% of subjects had antibodies capable of binding the RBD of Delta variant and no subject presented antibodies capable of binding the Omicron RBD antigen (Figure 4 b).

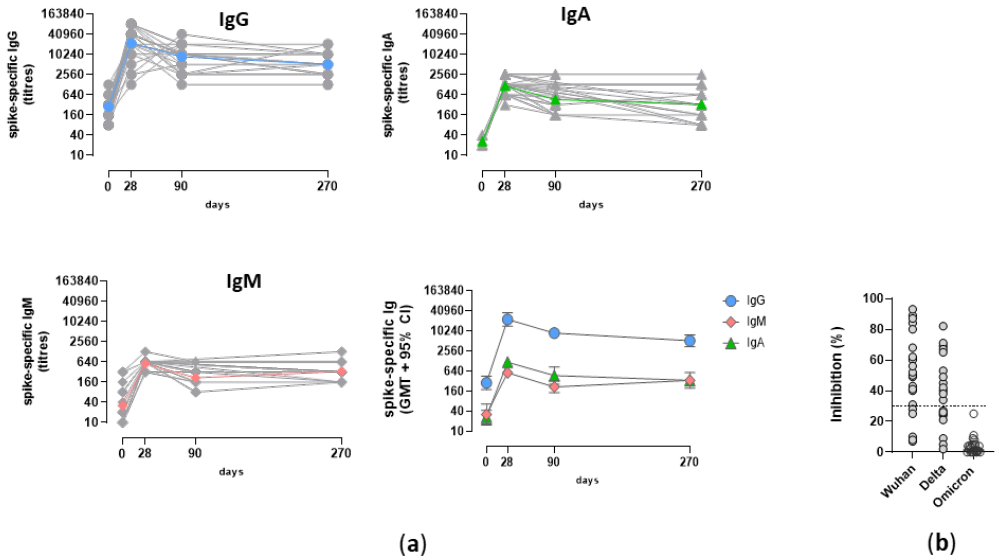

Figure 4. Spike-specific antibody response following SARS-CoV-2 mRNA vaccination. (**a**) Longitudinal analysis of spike specific IgG, IgA and IgM response in single subjects detected at baseline (0), 7 days (d7), 3 (M3) and 9 (M9) months after the second vaccine dose. The GMT value is colored in each graph. In the lower right panel, the GMT of the three antibody classes is shown. (**b**) Surrogate virus neutralization test performed at month 9 against the Wuhan, Delta and Omicron BA.1

 doi:10.20944/preprints202305.1190.v1

variants. Data are reported as ACE2/RBD binding inhibition percentage. The threshold (dotted black line) at 30% inhibition percentage discriminates between positive and negative sample.

4. Discussion

In this study we profiled the spike-specific B cell response upon two doses of the mRNA BNT162b2 vaccine in healthy individuals who had no documented history of infection. With a significant proportion of the global population still receiving only two doses of vaccination, there is an urgent need to investigate the durability of the memory response and its cross-reactivity with circulating viral variants. Studying the immune response to COVID-19 vaccines in the real-world setting is complicated by the overlap of recall responses from natural infection with new circulating variants, resulting in what is known as hybrid immunity. In this context, our study cohort represents a valuable group of healthy individuals whose SARS-CoV-2 specific immune response to vaccination has not been affected by the viral infection, as evidenced by the absence of antibodies against the viral nucleocapsid.

The immune response to vaccination typically involves the induction of antibody-secreting cells and serum immunoglobulins, as well as the generation of memory cells that can persist in the host for extended periods [48]. However, vaccination against SARS-CoV-2 has presented unique challenges due to the acute phase of the pandemic, mass vaccination efforts, and the use of new RNA-based vaccine technologies. The first objective of the anti-SARS-CoV-2 vaccine administration has been the induction of an effector antibody response capable to neutralize the virus in early stages of infection and contain its diffusion, with most studies relying on circulating antibody levels and neutralization activity [49,50]. These data have been particularly important, also considering the adoption, for the first time, of the novel RNA-based vaccine technology, nevertheless it is now well recognized the fundamental role of the immunological memory and the importance to investigate and characterize the B and T cellular responses. The duration of the memory response is a critical point that can vary depending on the vaccine or antigen. While previous reports have analysed the persistence of the spike-specific cellular response at 6 months post-immunization [21,24,31], here we profiled the spike-specific B cells trajectory from the initial effector phase (7 days after vaccination) up to 9 months, in the absence of natural infection. This is a particularly important point for studying the B cell immune response elicited by the primary cycle of mRNA vaccination without the confounding effects of hybrid immunity elicited by natural infection with SARS-CoV-2 or the impact of a booster dose. [25,51,52].

Multiparametric flow cytometry is highly effective in conducting in-depth analysis of immune responses following vaccination, as it enables measurement of the frequency, phenotype, and functional characteristics of antigen-specific cells [46]. To identify the different cellular phenotypes we integrated manual analysis of flow cytometry data with advanced automated tools [45]. S^+ RBD^+ B cells were clearly detected in blood 7 days after the second vaccine administration, and they continued to expand overtime, after a slow but not significant decline observed at month 3. This can be appreciated in the t-SNE analysis of the spike-specific B cells in the context of the total $CD19^{+/low}$ B cells performed at baseline, 7 days, 3 and 9 months after the second dose. It can be clearly observed that not only the amount of S^+ RBD^+B cells increased overtime, as reported also in other studies [23,31], but that their phenotype changed accordingly. The trajectory analysis of S^+RBD^+ B subsets highlighted a clear modulation of specific phenotypes overtime, with most of the metaclusters alternatively expressed at day 7 or month 9. The IgA^+ and IgG^+ plasmablasts were detected only immediately after vaccination, along with a pool of $CD21^-CD27^+$ IgA^+ and IgG^+ activated B cells and a small fraction of IgG^+ resting memory B cells. However, this scenario transformed over the subsequent weeks, with a reduction of activated B cells and an increase of the resting memory phenotype, positive for IgA or IgG. This is likely due to the transient downregulation of CD21 expression after vaccine administration associated with activated phenotype, and its return to higher levels in the subsequent weeks,

 doi:10.20944/preprints202305.1190.v1

as recently demonstrated also after influenza vaccination [53]. Resting memory B cells became the predominant subset at month 9, with a clear majority of IgG^+ switched cells, and a small fraction of unswitched (IgM^+ and IgD^+) B cells, as well.

DN/atypical IgG^+ $CD21^-CD27^-$ B cells were a small subset of spike-specific cells. Even though the DN population have been described as a dominant phenotype in many autoimmune disease [54], chronic infection such as HIV and malaria [55,56] and elderly [57], showing signs of exhaustion and dysfunction. Further studies however, have demonstrated that they represent a population planned to develop into plasmablasts and that even though $CD27^-$, DN cells show signatures of antigen experienced B cells, such as somatic hypermutation of their Ig genes [58]. Recently, they have been associated with an alternative lineage primed by primary vaccination and recalled by booster immunization [59]. As observed here, their expansion starts immediately after vaccine administration, peaks at month 3 and then declines overtime. IgG^+ MBC circulating at month 9 were able to reactivate and secrete spike-specific IgG, in most of the subjects.

Since the present study is a longitudinal analysis of the spike-specific B-cell response overtime, the analysis was performed on frozen/thawed cell samples. This procedure can result in partial damage to cell viability, particularly of the more fragile subtypes such as plasmablasts, thereby reducing the frequency of detectable antigen-specific cells. Nonetheless, the inclusion of $CD19^{low}$ cells in the parent gate is an important strategy to detect all the plasmablasts that have already downregulated CD19 expression.

Profiling the induction and persistence of spike-specific MBC in healthy subjects is of primary importance to allow for comparison with the response observed in fragile subjects characterized by an impaired immune system due to concomitant pathologies or immune aging [10,13,60,61]. Studies performed by our group in cohorts of fragile subjects, have shown that the behavior of the B cell response was different from that of healthy people. In myelofibrosis subjects and individuals transplanted with hematopoietic cells there was a lower and delayed B cell response [14,15], while people living with HIV generated a rate of spike-specific B cells comparable with healthy controls, but significantly different in phenotype, with a predominant double negative ($CD27^-$ IgD^-) profile [37]. Therefore, the different immune responsiveness to the same vaccine formulation among different cohorts of subjects, raises the necessity to carefully consider the vaccination schedules, including the necessity of booster doses, specifically tailored for the different category of subjects.

In our study we observed that spike-specific antibodies are still present 9 months after the first vaccination cycle, even though a physiological reduction of the median antibody titre respect to the peak, measured seven days after the second dose administration, was detected. As already observed in other studies [62], the stronger drop in antibody response occurred in the first two months after administration of the second dose (here observed between the time points d7 and month 3) but, thereafter, it remained at a relatively steady level up to 9 months in most of vaccinated subjects. Even if with differences in antibody levels, this trend was observed for IgG, IgA and IgM. The maintenance of circulating antibodies, especially IgG, 9 month after antigen stimulation can be due to antigen-specific long-lived plasma cells, generated within germinal centres upon vaccination with mRNA vaccines [36] and residing into the bone marrow. Concerning the antibody capacity of binding the spike protein and blocking its interaction with ACE-2 receptor, we observed that in 80% of subjects they bound the wild type protein, in 54% the Delta (B.1.617.2) variant, but no one recognized the Omicron (B.1.1.529). Studies of BCR repertoire have demonstrated that the frequency of B cell clones cross-reactive with the Omicron variant is about 10% of the bulk spike-specific B cells [63]; this could indirectly explain why the third dose, or breakthrough infection, significantly boosts the response to Omicron variant, as reported in other works [64–67] (Pastore *et al* in preparation).

In conclusion, this study allows to characterize the temporal dynamics and magnitude of the spike-specific B cell response in healthy subjects following the administration of the second dose of the BNT162b2 mRNA vaccine over a 9-month period.

5. Conclusions

Profiling the B cell response is of primary importance to design and refine vaccination schedules and policies tailored for healthy and fragile subjects. These results provide an important answer to the open question on the duration of the spike-specific memory response upon vaccination with two doses of the novel mRNA-based BNT162b2 vaccine in healthy subjects and provide a clear vision of the trajectory of antigen-specific B cell phenotypes. Since the future of RNA vaccines is very promising, and novel vaccines against other pathogens are in development, further data on the vaccine immunogenicity are of great relevance.

Supplementary Materials: The following supporting information can be downloaded at: www.mdpi.com/xxx/s1, Figure S1: Nucleoprotein-specific IgG;. Figure S2: Manual analysis of total B cells subsets.

Author Contributions: Conceptualization, Annalisa Ciabattini, Gabiria Pastore, Mario Tumbarello, Massimiliano Fabbiani, Francesca Montagnani and Donata Medaglini; Data curation, Simone Lucchesi and Giorgio Montesi; Formal analysis, Simone Lucchesi and Giorgio Montesi; Funding acquisition, Francesca Montagnani and Donata Medaglini; Investigation, Gabiria Pastore, Simone Costagli, Jacopo Polvere, Fabio Fiorino and Elena Pettini; Methodology, Annalisa Ciabattini, Gabiria Pastore and Francesca Montagnani; Project administration, Annalisa Ciabattini, Francesca Montagnani and Donata Medaglini; Resources, Arianna Lippi and Leonardo Ancillotti; Software, Simone Lucchesi and Giorgio Montesi; Supervision, Donata Medaglini; Writing – original draft, Annalisa Ciabattini; Writing – review & editing, Gabiria Pastore, Simone Lucchesi, Giorgio Montesi, Simone Costagli, Jacopo Polvere, Mario Tumbarello, Massimiliano Fabbiani, Francesca Montagnani and Donata Medaglini.

Funding: This research was supported by the Department of Medical Biotechnologies of the University of Siena (D.M.), and by Azienda Ospedaliera Universitaria Senese for the study insurance

Institutional Review Board Statement: The study was conducted in accordance with the Declaration of Helsinki, and approved by the local Ethical Committee for Clinical experimentation of Regione Toscana Area Vasta Sud Est (CEAVSE), protocol code 18869 IMMUNO_COV v1.0 of 18 November 2020, approved on the 21 December 2020.

Informed Consent Statement: Informed consent was obtained from all subjects involved in the study.

Data Availability Statement: The data presented in this study are available in this article (including in the Supplementary Materials).

Acknowledgments: We would like to thank all the healthy subjects who participated to the study, the Infectious and Tropical Diseases Unit Nursing team for collecting blood samples, Sara Zirpoli for technical assistance and Miriam Durante for the ethical approval procedures.

Conflicts of Interest: The authors declare no conflict of interest.

References

1. McDonald, I.; Murray, S.M.; Reynolds, C.J.; Altmann, D.M.; Boyton, R.J. Comparative Systematic Review and Meta-Analysis of Reactogenicity, Immunogenicity and Efficacy of Vaccines against SARS-CoV-2. *npj Vaccines* **2021**, *6*, 1–14, doi:10.1038/s41541-021-00336-1.
2. Villanueva, M.T. An MRNA Universal Vaccine for Influenza. *Nature Reviews Drug Discovery* **2023**, *22*, 98–98, doi:10.1038/d41573-023-00013-z.
3. NIH Launches Clinical Trial of Three MRNA HIV Vaccines | National Institutes of Health (NIH) Available online: https://www.nih.gov/news-events/news-releases/nih-launches-clinical-trial-three-mrna-hiv-vaccines (accessed on 12 May 2023).
4. Flemming, A. MRNA Vaccine Shows Promise in Autoimmunity. *Nat Rev Immunol* **2021**, *21*, 72–72, doi:10.1038/s41577-021-00504-3.
5. Rzymski, P.; Szuster-Ciesielska, A.; Dzieciątkowski, T.; Gwenzi, W.; Fal, A. MRNA Vaccines: The Future of Prevention of Viral Infections? *Journal of Medical Virology* **2023**, *95*, e28572, doi:10.1002/jmv.28572.

6. Feikin, D.R.; Higdon, M.M.; Abu-Raddad, L.J.; Andrews, N.; Araos, R.; Goldberg, Y.; Groome, M.J.; Huppert, A.; O'Brien, K.L.; Smith, P.G.; et al. Duration of Effectiveness of Vaccines against SARS-CoV-2 Infection and COVID-19 Disease: Results of a Systematic Review and Meta-Regression. *The Lancet* **2022**, *399*, 924–944, doi:10.1016/S0140-6736(22)00152-0.
7. Jung, J.; Sung, H.; Kim, S.-H. Covid-19 Breakthrough Infections in Vaccinated Health Care Workers. *N Engl J Med* **2021**, *385*, 1629–1630, doi:10.1056/NEJMc2113497.
8. Interim Statement on the Use of Additional Booster Doses of Emergency Use Listed MRNA Vaccines against COVID-19 Available online: https://www.who.int/news/item/17-05-2022-interim-statement-on-the-use-of-additional-booster-doses-of-emergency-use-listed-mrna-vaccines-against-covid-19 (accessed on 16 November 2022).
9. Ciabattini, A.; Garagnani, P.; Santoro, F.; Rappuoli, R.; Franceschi, C.; Medaglini, D. Shelter from the Cytokine Storm: Pitfalls and Prospects in the Development of SARS-CoV-2 Vaccines for an Elderly Population. *Semin Immunopathol* **2020**, *42*, 619–634, doi:10.1007/s00281-020-00821-0.
10. Ciabattini, A.; Nardini, C.; Santoro, F.; Garagnani, P.; Franceschi, C.; Medaglini, D. Vaccination in the Elderly: The Challenge of Immune Changes with Aging. *Semin Immunol* **2018**, *40*, 83–94, doi:10.1016/j.smim.2018.10.010.
11. Wang, X.; Han, M.; Fuentes, L.R.; Thwin, O.; Grobe, N.; Wang, K.; Wang, Y.; Kotanko, P. SARS-CoV-2 Neutralizing Antibody Response after Three Doses of MRNA1273 Vaccine and COVID-19 in Hemodialysis Patients. *Frontiers in Nephrology* **2022**, *2*.
12. Alidjinou, E.K.; Demaret, J.; Corroyer-Simovic, B.; Labreuche, J.; Goffard, A.; Trauet, J.; Lupau, D.; Miczek, S.; Vuotto, F.; Dendooven, A.; et al. Immunogenicity of BNT162b2 Vaccine Booster against SARS-CoV-2 Delta and Omicron Variants in Nursing Home Residents: A Prospective Observational Study in Older Adults Aged from 68 to 98 Years. *Lancet Reg Health Eur* **2022**, *17*, 100385, doi:10.1016/j.lanepe.2022.100385.
13. Corradini, P.; Agrati, C.; Apolone, G.; Mantovani, A.; Giannarelli, D.; Marasco, V.; Bordoni, V.; Sacchi, A.; Matusali, G.; Salvarani, C.; et al. Humoral and T-Cell Immune Response after Three Doses of MRNA SARS-CoV-2 Vaccines in Fragile Patients: The Italian VAX4FRAIL Study 2022, 2022.01.12.22269133.
14. Fiorino, F.; Ciabattini, A.; Sicuranza, A.; Pastore, G.; Santoni, A.; Simoncelli, M.; Polvere, J.; Galimberti, S.; Baratè, C.; Sammartano, V.; et al. The Third Dose of MRNA SARS-CoV-2 Vaccines Enhances the Spike-Specific Antibody and Memory B Cell Response in Myelofibrosis Patients. *Frontiers in Immunology* **2022**, *13*.
15. Pettini, E.; Ciabattini, A.; Pastore, G.; Polvere, J.; Lucchesi, S.; Fiorino, F.; Montagnani, F.; Bucalossi, A.; Tozzi, M.; Marotta, G.; et al. A Third Dose of MRNA-1273 Vaccine Improves SARS-CoV-2 Immunity in HCT Recipients with Low Antibody Response after 2 Doses. *Blood Adv* **2022**, bloodadvances.2021006599, doi:10.1182/bloodadvances.2021006599.
16. Watanabe, M.; Yakushijin, K.; Funakoshi, Y.; Ohji, G.; Ichikawa, H.; Sakai, H.; Hojo, W.; Saeki, M.; Hirakawa, Y.; Matsumoto, S.; et al. A Third Dose COVID-19 Vaccination in Allogeneic Hematopoietic Stem Cell Transplantation Patients. *Vaccines (Basel)* **2022**, *10*, 1830, doi:10.3390/vaccines10111830.
17. Kimura, M.; Ferreira, V.H.; Kothari, S.; Pasic, I.; Mattsson, J.I.; Kulasingam, V.; Humar, A.; Mah, A.; Delisle, J.-S.; Ierullo, M.; et al. Safety and Immunogenicity After a Three-Dose SARS-CoV-2 Vaccine Schedule in Allogeneic Stem Cell Transplant Recipients. *Transplant Cell Ther* **2022**, *28*, 706.e1-706.e10, doi:10.1016/j.jtct.2022.07.024.
18. Guerrini, G.; Magrì, D.; Gioria, S.; Medaglini, D.; Calzolai, L. Characterization of Nanoparticles-Based Vaccines for COVID-19. *Nat Nanotechnol* **2022**, *17*, 570–576, doi:10.1038/s41565-022-01129-w.
19. Mehrabi Nejad, M.-M.; Shobeiri, P.; Dehghanbanadaki, H.; Tabary, M.; Aryannejad, A.; Haji Ghadery, A.; Shabani, M.; Moosaie, F.; SeyedAlinaghi, S.; Rezaei, N. Seroconversion Following the First, Second, and Third Dose of SARS-CoV-2 Vaccines in Immunocompromised Population: A Systematic Review and Meta-Analysis. *Virol J* **2022**, *19*, 132, doi:10.1186/s12985-022-01858-3.
20. Choi, A.; Koch, M.; Wu, K.; Chu, L.; Ma, L.; Hill, A.; Nunna, N.; Huang, W.; Oestreicher, J.; Colpitts, T.; et al. Safety and Immunogenicity of SARS-CoV-2 Variant MRNA Vaccine Boosters in Healthy Adults: An Interim Analysis. *Nat Med* **2021**, *27*, 2025–2031, doi:10.1038/s41591-021-01527-y.
21. Goel, R.R.; Painter, M.M.; Apostolidis, S.A.; Mathew, D.; Meng, W.; Rosenfeld, A.M.; Lundgreen, K.A.; Reynaldi, A.; Khoury, D.S.; Pattekar, A.; et al. MRNA Vaccines Induce Durable Immune Memory to SARS-CoV-2 and Variants of Concern. *Science* **2021**, *374*, abm0829, doi:10.1126/science.abm0829.
22. Pettini, E.; Medaglini, D.; Ciabattini, A. Profiling the B Cell Immune Response Elicited by Vaccination against the Respiratory Virus SARS-CoV-2. *Frontiers in Immunology* **2022**, *13*.

23. Terreri, S.; Piano Mortari, E.; Vinci, M.R.; Russo, C.; Alteri, C.; Albano, C.; Colavita, F.; Gramigna, G.; Agrati, C.; Linardos, G.; et al. Persistent B Cell Memory after SARS-CoV-2 Vaccination Is Functional during Breakthrough Infections. *Cell Host Microbe* **2022**, *30*, 400-408.e4, doi:10.1016/j.chom.2022.01.003.
24. Kotaki, R.; Adachi, Y.; Moriyama, S.; Onodera, T.; Fukushi, S.; Nagakura, T.; Tonouchi, K.; Terahara, K.; Sun, L.; Takano, T.; et al. SARS-CoV-2 Omicron-Neutralizing Memory B Cells Are Elicited by Two Doses of BNT162b2 MRNA Vaccine. *Science Immunology* **2022**, *7*, eabn8590, doi:10.1126/sciimmunol.abn8590.
25. Andreano, E.; Paciello, I.; Piccini, G.; Manganaro, N.; Pileri, P.; Hyseni, I.; Leonardi, M.; Pantano, E.; Abbiento, V.; Benincasa, L.; et al. Hybrid Immunity Improves B Cells and Antibodies against SARS-CoV-2 Variants. *Nature* **2021**, *600*, 530–535, doi:10.1038/s41586-021-04117-7.
26. Hui, D.S. Hybrid Immunity and Strategies for COVID-19 Vaccination. *The Lancet Infectious Diseases* **2022**, *0*, doi:10.1016/S1473-3099(22)00640-5.
27. Akkaya, M.; Kwak, K.; Pierce, S.K. B Cell Memory: Building Two Walls of Protection against Pathogens. *Nat Rev Immunol* **2020**, *20*, 229–238, doi:10.1038/s41577-019-0244-2.
28. Palm, A.-K.E.; Henry, C. Remembrance of Things Past: Long-Term B Cell Memory After Infection and Vaccination. *Frontiers in Immunology* **2019**, *10*.
29. Papadopoulou, A.; Stavridou, F.; Giannaki, M.; Paschoudi, K.; Chatzopoulou, F.; Gavriilaki, E.; Georgolopoulos, G.; Anagnostopoulos, A.; Yannaki, E. Robust SARS-COV-2-Specific T-Cell Immune Memory Persists Long-Term in Immunocompetent Individuals Post BNT162b2 Double Shot. *Heliyon* **2022**, *8*, e09863, doi:10.1016/j.heliyon.2022.e09863.
30. Tarke, A.; Coelho, C.H.; Zhang, Z.; Dan, J.M.; Yu, E.D.; Methot, N.; Bloom, N.I.; Goodwin, B.; Phillips, E.; Mallal, S.; et al. SARS-CoV-2 Vaccination Induces Immunological T Cell Memory Able to Cross-Recognize Variants from Alpha to Omicron. *Cell* **2022**, *185*, 847-859.e11, doi:10.1016/j.cell.2022.01.015.
31. Zhang, Z.; Mateus, J.; Coelho, C.H.; Dan, J.M.; Moderbacher, C.R.; Gálvez, R.I.; Cortes, F.H.; Grifoni, A.; Tarke, A.; Chang, J.; et al. Humoral and Cellular Immune Memory to Four COVID-19 Vaccines. *Cell* **2022**, *185*, 2434-2451.e17, doi:10.1016/j.cell.2022.05.022.
32. Pušnik, J.; König, J.; Mai, K.; Richter, E.; Zorn, J.; Proksch, H.; Schulte, B.; Alter, G.; Streeck, H. Persistent Maintenance of Intermediate Memory B Cells Following SARS-CoV-2 Infection and Vaccination Recall Response. *J Virol 96*, e00760-22, doi:10.1128/jvi.00760-22.
33. Sette, A.; Crotty, S. Immunological Memory to SARS-CoV-2 Infection and COVID-19 Vaccines. *Immunological Reviews* **2022**, *310*, 27–46, doi:10.1111/imr.13089.
34. Sokal, A.; Chappert, P.; Barba-Spaeth, G.; Roeser, A.; Fourati, S.; Azzaoui, I.; Vandenberghe, A.; Fernandez, I.; Meola, A.; Bouvier-Alias, M.; et al. Maturation and Persistence of the Anti-SARS-CoV-2 Memory B Cell Response. *Cell* **2021**, *184*, 1201-1213.e14, doi:10.1016/j.cell.2021.01.050.
35. Ciabattini, A.; Pastore, G.; Fiorino, F.; Polvere, J.; Lucchesi, S.; Pettini, E.; Auddino, S.; Rancan, I.; Durante, M.; Miscia, M.; et al. *Evidence of SARS-Cov-2-Specific Memory B Cells Six Months after Vaccination with BNT162b2 MRNA Vaccine*; 2021; p. 2021.07.12.21259864;
36. Kim, W.; Zhou, J.Q.; Horvath, S.C.; Schmitz, A.J.; Sturtz, A.J.; Lei, T.; Liu, Z.; Kalaidina, E.; Thapa, M.; Alsoussi, W.B.; et al. Germinal Centre-Driven Maturation of B Cell Response to MRNA Vaccination. *Nature* **2022**, *604*, 141–145, doi:10.1038/s41586-022-04527-1.
37. Polvere, J.; Fabbiani, M.; Pastore, G.; Rancan, I.; Rossetti, B.; Durante, M.; Zirpoli, S.; Morelli, E.; Pettini, E.; Lucchesi, S.; et al. B Cell Response Six Months after SARS-CoV-2 MRNA Vaccination in People Living with HIV under Antiretroviral Therapy 2022, 2022.07.01.22277132.
38. Hahne, F.; LeMeur, N.; Brinkman, R.R.; Ellis, B.; Haaland, P.; Sarkar, D.; Spidlen, J.; Strain, E.; Gentleman, R. FlowCore: A Bioconductor Package for High Throughput Flow Cytometry. *BMC Bioinformatics* **2009**, *10*, 106, doi:10.1186/1471-2105-10-106.
39. Parks, D.R.; Roederer, M.; Moore, W.A. A New "Logicle" Display Method Avoids Deceptive Effects of Logarithmic Scaling for Low Signals and Compensated Data. *Cytometry Part A* **2006**, *69A*, 541–551, doi:10.1002/cyto.a.20258.
40. van der Maaten, L.; Hinton, G. Viualizing Data Using T-SNE. *Journal of Machine Learning Research* **2008**, *9*, 2579–2605.

41. Van Gassen, S.; Callebaut, B.; Van Helden, M.J.; Lambrecht, B.N.; Demeester, P.; Dhaene, T.; Saeys, Y. FlowSOM: Using Self-Organizing Maps for Visualization and Interpretation of Cytometry Data. *Cytometry A* **2015**, *87*, 636–645, doi:10.1002/cyto.a.22625.
42. Dai, Y.; Xu, A.; Li, J.; Wu, L.; Yu, S.; Chen, J.; Zhao, W.; Sun, X.-J.; Huang, J. CytoTree: An R/Bioconductor Package for Analysis and Visualization of Flow and Mass Cytometry Data. *BMC Bioinformatics* **2021**, *22*, 138, doi:10.1186/s12859-021-04054-2.
43. Leek, J.T.; Johnson, W.E.; Parker, H.S.; Jaffe, A.E.; Storey, J.D. The Sva Package for Removing Batch Effects and Other Unwanted Variation in High-Throughput Experiments. *Bioinformatics* **2012**, *28*, 882–883, doi:10.1093/bioinformatics/bts034.
44. Malek, M.; Taghiyar, M.J.; Chong, L.; Finak, G.; Gottardo, R.; Brinkman, R.R. FlowDensity: Reproducing Manual Gating of Flow Cytometry Data by Automated Density-Based Cell Population Identification. *Bioinformatics* **2015**, *31*, 606–607, doi:10.1093/bioinformatics/btu677.
45. Lucchesi, S.; Furini, S.; Medaglini, D.; Ciabattini, A. From Bivariate to Multivariate Analysis of Cytometric Data: Overview of Computational Methods and Their Application in Vaccination Studies. *Vaccines (Basel)* **2020**, *8*, doi:10.3390/vaccines8010138.
46. Lucchesi, S.; Nolfi, E.; Pettini, E.; Pastore, G.; Fiorino, F.; Pozzi, G.; Medaglini, D.; Ciabattini, A. Computational Analysis of Multiparametric Flow Cytometric Data to Dissect B Cell Subsets in Vaccine Studies. *Cytometry A* **2020**, *97*, 259–267, doi:10.1002/cyto.a.23922.
47. Tan, C.W.; Chia, W.N.; Qin, X.; Liu, P.; Chen, M.I.-C.; Tiu, C.; Hu, Z.; Chen, V.C.-W.; Young, B.E.; Sia, W.R.; et al. A SARS-CoV-2 Surrogate Virus Neutralization Test Based on Antibody-Mediated Blockage of ACE2–Spike Protein–Protein Interaction. *Nat Biotechnol* **2020**, *38*, 1073–1078, doi:10.1038/s41587-020-0631-z.
48. Sallusto, F.; Lanzavecchia, A.; Araki, K.; Ahmed, R. From Vaccines to Memory and Back. *Immunity* **2010**, *33*, 451–463, doi:10.1016/j.immuni.2010.10.008.
49. Khoury, D.S.; Cromer, D.; Reynaldi, A.; Schlub, T.E.; Wheatley, A.K.; Juno, J.A.; Subbarao, K.; Kent, S.J.; Triccas, J.A.; Davenport, M.P. Neutralizing Antibody Levels Are Highly Predictive of Immune Protection from Symptomatic SARS-CoV-2 Infection. *Nat Med* **2021**, *27*, 1205–1211, doi:10.1038/s41591-021-01377-8.
50. Krammer, F. A Correlate of Protection for SARS-CoV-2 Vaccines Is Urgently Needed. *Nat Med* **2021**, *27*, 1147–1148, doi:10.1038/s41591-021-01432-4.
51. Buckner, C.M.; Kardava, L.; Merhebi, O.E.; Narpala, S.R.; Serebryannyy, L.; Lin, B.C.; Wang, W.; Zhang, X.; Assis, F.L. de; Kelly, S.E.M.; et al. Interval between Prior SARS-CoV-2 Infection and Booster Vaccination Impacts Magnitude and Quality of Antibody and B Cell Responses. *Cell* **2022**, *185*, 4333-4346.e14, doi:10.1016/j.cell.2022.09.032.
52. Rodda, L.B.; Morawski, P.A.; Pruner, K.B.; Fahning, M.L.; Howard, C.A.; Franko, N.; Logue, J.; Eggenberger, J.; Stokes, C.; Golez, I.; et al. Imprinted SARS-CoV-2-Specific Memory Lymphocytes Define Hybrid Immunity. *Cell* **2022**, *185*, 1588-1601.e14, doi:10.1016/j.cell.2022.03.018.
53. Andrews, S.F.; Chambers, M.J.; Schramm, C.A.; Plyler, J.; Raab, J.E.; Kanekiyo, M.; Gillespie, R.A.; Ransier, A.; Darko, S.; Hu, J.; et al. Activation Dynamics and Immunoglobulin Evolution of Pre-Existing and Newly Generated Human Memory B Cell Responses to Influenza Hemagglutinin. *Immunity* **2019**, *51*, 398-410.e5, doi:10.1016/j.immuni.2019.06.024.
54. Wei, C.; Anolik, J.; Cappione, A.; Zheng, B.; Pugh-Bernard, A.; Brooks, J.; Lee, E.-H.; Milner, E.C.B.; Sanz, I. A New Population of Cells Lacking Expression of CD27 Represents a Notable Component of the B Cell Memory Compartment in Systemic Lupus Erythematosus. *J Immunol* **2007**, *178*, 6624–6633, doi:10.4049/jimmunol.178.10.6624.
55. Moir, S.; Ho, J.; Malaspina, A.; Wang, W.; DiPoto, A.C.; O'Shea, M.A.; Roby, G.; Kottilil, S.; Arthos, J.; Proschan, M.A.; et al. Evidence for HIV-Associated B Cell Exhaustion in a Dysfunctional Memory B Cell Compartment in HIV-Infected Viremic Individuals. *Journal of Experimental Medicine* **2008**, *205*, 1797–1805, doi:10.1084/jem.20072683.
56. Weiss, G.E.; Crompton, P.D.; Li, S.; Walsh, L.A.; Moir, S.; Traore, B.; Kayentao, K.; Ongoiba, A.; Doumbo, O.K.; Pierce, S.K. Atypical Memory B Cells Are Greatly Expanded in Individuals Living in a Malaria-Endemic Area. *The Journal of Immunology* **2009**, *183*, 2176–2182, doi:10.4049/jimmunol.0901297.
57. Colonna-Romano, G.; Bulati, M.; Aquino, A.; Pellicanò, M.; Vitello, S.; Lio, D.; Candore, G.; Caruso, C. A Double-Negative (IgD-CD27-) B Cell Population Is Increased in the Peripheral Blood of Elderly People. *Mech Ageing Dev* **2009**, *130*, 681–690, doi:10.1016/j.mad.2009.08.003.

58. Ehrhardt, G.R.A.; Hsu, J.T.; Gartland, L.; Leu, C.-M.; Zhang, S.; Davis, R.S.; Cooper, M.D. Expression of the Immunoregulatory Molecule FcRH4 Defines a Distinctive Tissue-Based Population of Memory B Cells. *Journal of Experimental Medicine* **2005**, *202*, 783–791, doi:10.1084/jem.20050879.
59. Sutton, H.J.; Aye, R.; Idris, A.H.; Vistein, R.; Nduati, E.; Kai, O.; Mwacharo, J.; Li, X.; Gao, X.; Andrews, T.D.; et al. Atypical B Cells Are Part of an Alternative Lineage of B Cells That Participates in Responses to Vaccination and Infection in Humans. *Cell Reports* **2021**, *34*, doi:10.1016/j.celrep.2020.108684.
60. Fiorino, F.; Sicuranza, A.; Ciabattini, A.; Santoni, A.; Pastore, G.; Simoncelli, M.; Polvere, J.; Galimberti, S.; Auddino, S.; Baratè, C.; et al. The Slower Antibody Response in Myelofibrosis Patients after Two Doses of MRNA SARS-CoV-2 Vaccine Calls for a Third Dose. *Biomedicines* **2021**, *9*, 1480, doi:10.3390/biomedicines9101480.
61. Ruggeri, E.M.; Nelli, F.; Giannarelli, D.; Fabbri, A.; Giron Berrios, J.R.; Virtuoso, A.; Marrucci, E.; Mazzotta, M.; Schirripa, M.; Signorelli, C.; et al. Dynamic Changes in Peripheral Lymphocytes and Antibody Response Following a Third Dose of SARS-CoV-2 MRNA-BNT162b2 Vaccine in Cancer Patients. *Sci Rep* **2022**, *12*, 21908, doi:10.1038/s41598-022-25558-8.
62. Notarte, K.I.; Guerrero-Arguero, I.; Velasco, J.V.; Ver, A.T.; Santos de Oliveira, M.H.; Catahay, J.A.; Khan, M.S.R.; Pastrana, A.; Juszczyk, G.; Torrelles, J.B.; et al. Characterization of the Significant Decline in Humoral Immune Response Six Months Post-SARS-CoV-2 MRNA Vaccination: A Systematic Review. *J Med Virol* **2022**, *94*, 2939–2961, doi:10.1002/jmv.27688.
63. Sokal, A.; Broketa, M.; Barba-Spaeth, G.; Meola, A.; Fernández, I.; Fourati, S.; Azzaoui, I.; Selle, A. de L.; Vandenberghe, A.; Roeser, A.; et al. Analysis of MRNA Vaccination-Elicited RBD-Specific Memory B Cells Reveals Strong but Incomplete Immune Escape of the SARS-CoV-2 Omicron Variant. *Immunity* **2022**, *55*, 1096-1104.e4, doi:10.1016/j.immuni.2022.04.002.
64. Munro, A.P.S.; Janani, L.; Cornelius, V.; Aley, P.K.; Babbage, G.; Baxter, D.; Bula, M.; Cathie, K.; Chatterjee, K.; Dodd, K.; et al. Safety and Immunogenicity of Seven COVID-19 Vaccines as a Third Dose (Booster) Following Two Doses of ChAdOx1 NCov-19 or BNT162b2 in the UK (COV-BOOST): A Blinded, Multicentre, Randomised, Controlled, Phase 2 Trial. *The Lancet* **2021**, *398*, 2258–2276, doi:10.1016/S0140-6736(21)02717-3.
65. Garcia-Beltran, W.F.; St Denis, K.J.; Hoelzemer, A.; Lam, E.C.; Nitido, A.D.; Sheehan, M.L.; Berrios, C.; Ofoman, O.; Chang, C.C.; Hauser, B.M.; et al. MRNA-Based COVID-19 Vaccine Boosters Induce Neutralizing Immunity against SARS-CoV-2 Omicron Variant. *Cell* **2022**, *185*, 457-466.e4, doi:10.1016/j.cell.2021.12.033.
66. Muik, A.; Lui, B.G.; Wallisch, A.-K.; Bacher, M.; Mühl, J.; Reinholz, J.; Ozhelvaci, O.; Beckmann, N.; Güimil Garcia, R. de la C.; Poran, A.; et al. Neutralization of SARS-CoV-2 Omicron by BNT162b2 MRNA Vaccine-Elicited Human Sera. *Science* **2022**, *375*, 678–680, doi:10.1126/science.abn7591.
67. Goel, R.R.; Painter, M.M.; Lundgreen, K.A.; Apostolidis, S.A.; Baxter, A.E.; Giles, J.R.; Mathew, D.; Pattekar, A.; Reynaldi, A.; Khoury, D.S.; et al. Efficient Recall of Omicron-Reactive B Cell Memory after a Third Dose of SARS-CoV-2 MRNA Vaccine. *Cell* **2022**, *185*, 1875-1887.e8, doi:10.1016/j.cell.2022.04.009.